DOI: https://doi.org/10.15276/hait.09.2026.17
UDC 621.233:629.113.65:519.87

Computer simulation of an electric bicycle wheel drive with real load emulation

Ihor Z. Shchur[1)]
ORCID: https://orcid.org/0000-0001-7346-1463; ihor.z.shchur@lpnu.ua. Scopus Author ID: 36348908300
Ihor Y. Lutchyn[1)]
ORCID: https://orcid.org/0009-0003-2691-9381; ihor.y.lutchyn@lpnu.ua
Mariusz Korkosz[2)]
ORCID: https://orcid.org/0000-0002-9097-0988; mkosz@prz.edu.pl. Scopus Author ID: 56567985000
[1)] Lviv Polytechnic National University, 12, Stepana Bandery Str. Lviv, 79013, Ukraine
[2)] Rzeszow University of Technology, 12, Aleja Powstańców Warszawy. Rzeszow, 35-029, Poland

ABSTRACT

Topicality. Micro-mobile electric vehicles, whose drives are based on brushless DC motors, have become widespread in the last decade. The features of the electric drive systems of these vehicles and their on-board power supply systems are the subject of scientific research aimed at solving such key problems as: increasing the driving range, reducing electromagnetic torque ripple, improving the efficiency of regenerative braking, etc. A review of the literature shows that solving each individual problem involves two different approaches: computer simulation and physical experimentation. **Purpose and objectives.** To combine both approaches of testing: conducting experimental research with real vehicle systems and simulating the effect of road load and real dynamic load on the drive in transient modes using a corresponding load emulator. The latter consists of hardware that generates mechanical load on the drive and software that allows simulating various specified and repeated vehicle motion modes in experiments. **Methods.** In this work, the Hardware-In-The-Loop approach is applied to an electric bicycle test bench, in which a real wheel with in-wheel motor is connected via a friction transmission to a DC loading machine controlled by a two-quadrant DC-DC converter. **Results.** In this work, to control the torque of the loading machine, an emulator control system structure was developed, in which the conditions for the movement of the electric bicycle are set and tasks related to these conditions are formed for static and dynamic loads. A computer model of a test bench for studying the electric bicycle drive, developed in the Matlab/Simulink environment, made it possible to identify the features of the hardware part of the in-wheel motor load emulator. In particular, during the emulation of a dynamic load associated with the high moment of inertia of the drive, when the electric bicycle starts and initially accelerates at low speeds, the two-quadrant DC-DC converter is unable to provide the required value of the braking current of the load machine. Therefore, it was necessary to ensure the operation of the DC-DC converter in the third quadrant for the specified mode using an additionally introduced two-transistor switch, which allows switching the operation of the DC-DC converter from the second to the third quadrant and vice versa. A control system has been developed that performs such switching. **Conclusions.** A comparison of the results of computer simulation of the operation of the electric bicycle in-wheel motor drive on a test bench with load emulation with the corresponding results of simulation of the operation of the same drive in an electric bicycle under the same driving conditions showed a discrepancy in the main motion coordinates of no more than of seven percent, which confirms the adequacy of the emulation and the operability of all solutions adopted for the creation of the test bench.

Keywords: Electric bicycle; test bench; physical model of an electric drive; brushless DC motor; real load emulator; computer model

For citation: **Shchur I. Z., Lutchyn I. Y., Korkosz M. "Computer simulation of an electric bicycle wheel drive with real load emulation". *Herald of Advanced Information Technology*. 2026; Vol. 9 No. 2: 247–260. DOI: https://doi.org/10.15276/hait.09.2026.17**

INTRODUCTION

Micro-mobile electric vehicles (MEVs), such as electric scooters, electric bicycles (EBs), segways, monowheels, etc., are considered a viable and inexpensive alternative to cars for short trips in urban areas [1]. In Ukraine, according to the Law No. 3220-IX of 30.06.2023, MEVs are recognized as road users, and for the lightest ones (up to 25 km/h and up to 1000 W), no license or registration is required.

Such MEVs have their own structural features due to their required low weight and low cost. However, these features should not limit the requirements for high consumer indicators of MEVs, which include high efficiency [2] that ensures the necessary range, and high reliability and safety during operation, which in general still remains at a low level [3]. To meet all these requirements, new technical solutions are needed, which necessitates ongoing scientific research, for which a modern research base must be created. This paper presents the features of the design and development of the control system of test bench for researching of EB drives based on software emulation of real static and dynamic loads. The verification of the proposed solutions is confirmed by the results of computer simulation.

© Shchur I., Lutchyn I., Korkosz M., 2026

This is an open access article under the CC BY license (http://creativecommons.org/licenses/by/4.0/deed.uk)

LITERATURE REVIEW AND PROBLEM STATEMENT

MEV powertrain systems are designed for maximum simplicity and low cost using the simplest configuration: the power supply subsystem consists of a lithium battery (B), and the traction electric drive subsystem is based on a brushless DC (BLDC) motor that operates only in a traction mode [4]. However, the problems of increasing the range and reliability of operation have led to research and development aimed at improving key subsystems and increasing their efficiency [5], [6].

Many researchers are interested in the issue of regenerative braking and increasing its efficiency. In particular, in [7], it was proposed to use the reverse conductivity of field-effect transistors instead of freewheeling diodes to return electrical energy to the battery during a pulse width modulation (PWM) pause. Depending on the selected braking method, this approach provides an increase in the efficiency of a power converter from 3.5 % to 10 %. Another problem of regeneration is braking at low speeds. The authors of [8] proposed a type II modular system with a current controller to ensure a higher value of the EMF amplification factor of a DC-DC converter for battery recharging. Other authors focused their attention on the implementation of universal power supply converters that perform traction, regenerative braking, battery charging, and other tasks [9], and on demonstrating the advantages of using bipolar PWM to improve the quality of BLDC motor control [10]. Article [11] is devoted to a review and analysis of the latest developments in the field of bidirectional semiconductor converters, including an assessment of their various topologies, a discussion of ways to optimize braking force and the amount of recovered energy. A study of the limitations of regenerative braking of electric traction vehicles and their drive circuits, taking into account the nonlinear parameters of the circuit and variations in the internal resistance of the AB, was presented in [12]. Using a detailed model of the circuit, the authors managed to achieve an 8.73% increase in the efficiency of regenerative braking when using the lead-acid battery. Other authors focused on the use of bidirectional Zeta–SEPIC converters in braking energy recovery systems [13].

Practical experience shows that vehicles often require rapid acceleration and/or braking, which are harmful processes for battery. Since modes of rapid energy accumulation and release are operational for supercapacitor (SC) modules, hybrid B-SC power supply systems have recently become increasingly popular [14], [15]. It is often proposed to add some additional functions to these systems: current stabilization (electromagnetic torque of the motor) using a step-down DC-DC converter [14]; use of specialized control algorithms for the regeneration system operating on the SC module [15]. Other authors have focused their efforts on researching the advantages of SCs in a hybrid energy storage system using the MATLAB/Simulink software environment [16] and AVL Cruise software environment, taking into account real driving conditions with standard and advanced control algorithms for the on-board power supply system [17]. Other works were aimed at studying the joint operation of the SC module and the B in regenerative braking systems, identifying the advantages of their joint operation, as well as energy efficiency [18], the use of modular BLDC motors in traction systems [19], and special configurations of BLDC motors with a hybrid on-board power supply system [20].

Another equally important problem of MEVs is the electromagnetic torque ripple of the BLDC motors caused by the non-sinusoidal nature of the back EMF, the discrete nature of the armature winding commutation, and the design features of the above-mentioned motors [21]. In this area, the authors focused on such aspects as: a review of technologies for reducing BLDC motor torque ripple [21], development of a strategy to reduce ripple using a Zeta converter [22], development of a new commutation method that evaluates the commutation angle error in real time with its integration into the direct torque control (DTC) method [23].

Traditionally, research aimed at developing new solutions, creating new technical means, or improving existing ones is divided into two stages:

1) the theoretical part, which consists of creating mathematical models that are further implemented in the form of computer models on which simulation studies are conducted;

2) the practical part, which consists of creating mock-ups or experimental samples of new technology, which are used to conduct experimental research.

The theoretical part, given the current developments in all areas of science and the possibilities of computer modeling, has very broad opportunities. However, in order to verify the theoretical results obtained, a practical part is necessary, which is accompanied by significant financial and time costs. In addition to these problems, experimental research has such disadvantages as the complexity of reproducing and

ISSN 2663-0176 (Print)
ISSN 2663-7731 (Online)

repeating the necessary research conditions. This is partially compensated by conducting cycles of similar studies with subsequent statistical processing of the results obtained.

Recently, the two-stage paradigm of research and development described above has undergone changes in the direction of integrating these two stages. The new research methodology has been named Hardware-in-the-Loop (HIL) [24]. HIL combines real physical hardware that operates in a virtual environment simulated by software, moreover the hardware interacting with the virtual environment as it would with a real one. Initially, HIL was used to test real control systems for modeled objects. This was particularly useful in cases of dangerous or expensive real objects, such as controlling a thermal power plant generator [25]. Nowadays, the HIL method is used more widely and flexibly, combining hardware and software subsystems in various combinations for different purposes in a single complex. This approach has led to the development of an even newer simulation technology – digital twins [26].

Article [27] presents the concept and features of the HIL approach, as well as the main principles of dynamic emulation of mechanical loads of electric drives, such as: emulation with a compensator and tracking controller, emulation based on nonlinear control, and emulation with predictive compensation. In addition, the authors demonstrated emulation based on nonlinear control using the example of a pendulum. Unlike existing methods of dynamic load torque emulation, the method presented in [28] is simplified, especially in terms of parameter tuning. The operation of this method is limited by a certain bandwidth, especially if the parameters of inertia and viscous friction of the mechanism are not well known, but it is suitable for emulating a wide range of load mechanisms. The authors of article [29] proposed and demonstrated the emulation of lithium-ion battery cells. With the help of the developed device, the dynamic electrical behavior of any battery cell can be emulated with minor deviations from the behavior of a real battery.

RESEARCH AIM AND OBJECTIVES

This paper proposes the development of a HIL testing system for researching the operation of the main subsystems of modern EB. To this end, it is necessary to create a test bench with physically implemented subsystems of electric drive and power supply, and to test them under repeatable specified conditions of real EB movement with a passenger, use an emulator of real static and dynamic load of the drive wheel with an electric motor. The emulator will consist of hardware in the form of a loading electric machine controlled by a semiconductor converter, and software that generates a load on the wheel according to the trajectory specified by the passenger-driver and the specified road conditions. Such a system will enable research aimed at solving urgent problems related to improving the performance of EB. The first step in creating a HIL system for testing EB is its computer modeling and research, which will provide answers to the main aspects of building an emulator of real static and dynamic loads.

DESCRIPTION OF THE STAND FOR TESTING THE DRIVE OF AN ELECTRIC BICYCLE

Fig. 1 shows a sketch of a test bench for studying the EB drive. The wheel 1 with the integrated BLDC in-wheel motor 2 is mounted on supports 6, which are attached to the base 8. The friction transmission between the wheel and the DC loading machine (LM) 3 is carried out using a drum 4 installed on the LM shaft. One end of this drum's axle is fixed in a bearing on a support 7, which is attached to the base 8. The EB controls are located on the steering wheel 5.

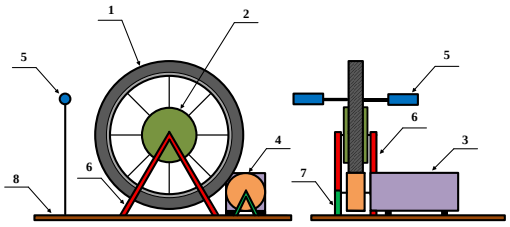


Fig. 1. **Sketch of the EB drive test bench**
***Source*: compiled by the authors**

Fig. 2 shows a functional diagram of the test bench (its main parameters are given in Table 1), which consists of two parts: an EB drive and a dynamic and static road load emulator.

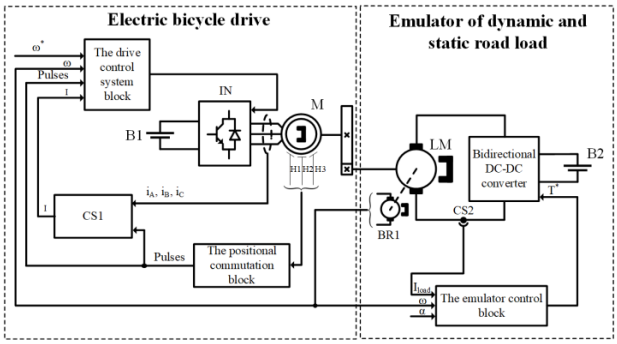


Fig. 2. **Functional diagram of the stand**
***Source*: compiled by the authors**

Table 1. **Stand parameters**

Parameter	Value
Wheel radius	0.329 m
LM drum radius	0.074 m
Friction transmission coefficient	4.44
Coefficient of viscous friction	0.05 N·m·s
Total moment of inertia reduced to the BLDC motor shaft	0.5 kg·m^2

***Source*: compiled by the authors**

The BLDC in-wheel motor with permanent magnets (PM) M (parameters are given in Table 2) is powered by the battery B1 through a three-phase transistor bridge voltage inverter (IN). The positional commutation block is used to generate pulses necessary for switching IN transistors based on information from Hall sensors H1, H2, H3. The drive control system block implements a dual-loop cascade control system of the BLDC motor in traction and regenerative braking modes. The current sensor CS1 is used to obtain a DC signal I based on the BLDC motor linear currents and IN switching algorithms [30]. The LM (parameters are given in Table 3), in turn, is powered by the battery B2 through the bidirectional DC-DC converter. The emulator control block generates a load torque setpoint signal for the LM and implements the LM current (torque) control system based on information from the LM current sensor CS2. The tachogenerator BR1 is used as an LM angular velocity sensor.

Table 2. **BLDC motor parameters**

Parameter	Value
Rated power	500 W
Rated DC-bus voltage	48 V
Rated speed	250 rpm
Rated torque	20 N·m
Number of pole pairs	22
Phase resistance	0.317 Ω
Phase inductance	0.238 mH
Flux linkage (one pair of PM)	0.04 V·s

***Source*: compiled by the authors**

DYNAMIC EMULATION OF THE LOAD TORQUE OF AN ELECTRIC BICYCLE WHEEL

The equations of EB dynamics with a passenger, reduced to the axis of the BLDC in-wheel motor, are as follows [28]:

$$\alpha_{\text{BLDC.EB}} = J_{\text{EB}}^{-1}(T_{\text{BLDC.EB}} - T_{\text{load.EB}} - \\ -B_{\text{EB}}\omega_{\text{BLDC.EB}}), \quad (1)$$

$$\alpha_{\text{BLDC.EB}} = \frac{\mathrm{d}\omega_{\text{BLDC.EB}}}{\mathrm{d}t}, \quad (2)$$

where $\alpha_{\text{BLDC.EB}}$ is the angular acceleration of the BLDC motor of the EB with passenger, J_{EB} is the total moment of inertia of the EB with a passenger reduced to the BLDC motor shaft, $T_{\text{BLDC.EB}}$ is the torque developed by the EB's BLDC motor, $T_{\text{load.EB}}$ is the torque of the road load, B_{EB} is the coefficient of viscous friction of the EB`s in-wheel motor, and $\omega_{\text{BLDC.EB}}$ is the angular velocity of the EB's BLDC motor.

Table 3. **Parameters of LM**

Parameter	Value
Rated power	500 W
Rated voltage	60 V
Rated speed	1000 rpm
Rated torque	4.7 N·m
Armature resistance	1.19 Ω
Armature inductance	5 mH
Back-EMF constant	0.052 V·s
Torque constant	0.456 N·m/A

***Source*: compiled by the authors**

The solution of equations (1) and (2) with obtaining the angular velocity of the BLDC motor at the output is shown in the left highlighted part of the block diagram in Fig. 3 in the frame “Electric bicycle dynamics model”.

Similar to (1) and (2), equations can be constructed to describe the dynamics of the stand for EB research shown in Fig. 1:

$$\alpha_{\text{BLDC.st}} = J_{\text{st}}^{-1}(T_{\text{BLDC.st}} - i\,T_{\text{LM}} - \\ -B_{\text{st}}\omega_{\text{BLDC.st}}), \quad (3)$$

$$\alpha_{\text{BLDC.st}} = \frac{\mathrm{d}\omega_{\text{BLDC.st}}}{\mathrm{d}t}, \quad (4)$$

where $\alpha_{\text{BLDC.st}}$ is the angular acceleration of the BLDC motor in the stand, J_{st} is the total moment of inertia of the stand reduced to the in-wheel motor`s shaft, $T_{\text{BLDC.st}}$ is the torque developed by the BLDC motor of the stand, i is the ratio of the friction transmission between the wheel and the LM drum, T_{LM} is the LM torque, B_{st} is the the coefficient of viscous friction of the standw reduced to the in-wheel motor shaft, and $\omega_{\text{BLDC.st}}$ is the angular velocity of the stand`s BLDC motor.

The solution of equations (3) and (4) with obtaining the angular velocity of the BLDC motor of the stand is shown in the right highlighted part of the block diagram in Fig. 3 in the frame “Model of the stand dynamics.”

ISSN 2663-0176 (Print)
ISSN 2663-7731 (Online)

In order to adequately emulate the total static and dynamic load in a real EB using LM, the following equalities must be ensured in equations (1)-(4):

$$T_{\text{BLDC.st}} = T_{\text{BLDC.EB}} = T_{\text{BLDC}}, \quad (5)$$

$$\alpha_{\text{BLDC.st}} = \alpha_{\text{BLDC.EB}} = \alpha_{\text{BLDC}}, \quad (6)$$

$$\omega_{\text{BLDC.st}} = \omega_{\text{BLDC.EB}} = \omega_{\text{BLDC}}. \quad (7)$$

To ensure equality (5) in the block diagram in Fig. 3, the stand model uses the torque at the output of the stand's BLDC motor $T_{\text{BLDS.st}}$, while the load emulator uses the torque of the EB's BLDC motor $T_{\text{BLDS.EB}}$ from the motor torque setpoint signal on the output of the BLDC motor speed controller, as it has practically no ripple caused by discrete transistor switching. In order to ensure equalities (6) and (7), automatic control of the angular velocity of the stand in-wheel motor is used in the emulator block diagram. For this purpose, at the input of the proportional speed regulator SR, the values of the real angular velocity of the stand in-wheel motor and $\omega_{\text{BLDC.st}}$ are compared with the angular velocity of the in-wheel motor of the real EB, which is obtained at the output of the model of its dynamics $\omega_{\text{BLDC.EB}}$. At the output of the SR, a torque setpoint is formed, which in dynamic processes corrects the LM torque, and in steady states should be equal to zero, which will indicate that equations (6) and (7) are satisfied.

From equation (3), the torque formed by the emulator on the LM shaft with respect to equalities (5)-(7) will be as follows:

$$T_{\text{LM}} = i^{-1}(T_{\text{BLDC}} - \alpha_{\text{BLDC}} J_{st} - \\ - B_{\text{st}} \omega_{\text{BLDC}}). \quad (8)$$

The obtained equation (8), which describes the law of formation of the torque setpoint for the LM, is reflected in the "Load Emulator" model in the block diagram in Fig. 3. A similar expression is obtained in [28].

The expression for finding the road load torque is as follows:

$$T_{\text{load.EB}} = F_{\text{load.EB}} r_{\text{w}}, \quad (9)$$

where $F_{\text{load.EB}}$ is the resistance force of the EB motion and r_{w} is the EB wheel radius.

$F_{\text{load.EB}}$ consists of the forces required to overcome the rolling resistance F_{roll}, aerodynamic drag of air during EB movement F_{drag}, and the force caused by uphill movement F_{hill}:

$$F_{\text{load.EB}} = F_{\text{roll}} + F_{\text{drag}} + F_{\text{hill}}. \quad (10)$$

These forces are described by the following equations:

$$F_{\text{roll}} = \begin{cases} f_{\text{d}}\, m\, g \cos\gamma, & \omega > 0 \\ 0, & \omega = 0 \end{cases}, \quad (11)$$

$$F_{\text{drag}} = 0.5\, \rho_{\text{a}}\, A_{\text{f}}\, c_{\text{d}}\, v^2, \quad (12)$$

$$F_{\text{hill}} = m\, g \sin\alpha, \quad (13)$$

where m is the total mass of the EB with driver, γ is test angle of road ascent/descent, f_{d} is the rolling resistance coefficient, ρ_{a} is the air density, A_{f} is the frontal area of the EB with driver, c_{d} is the aerodynamic drag coefficient of EB with driver, and $v = r_{\text{w}}\omega$ is the EB speed.

The total moment of inertia of the EB with driver reduced to the BLDC motor shaft is equal to:

$$J_{\text{EB}} = k\, m\, r_{\text{w}}^2, \quad (14)$$

where k is a coefficient that takes into account the additional moment of inertia from the rotating parts of the system (two wheels).

Some of the main parameters of the equations for determining the road load torque $T_{\text{load.EB}}$ are taken from [31] and are given in Table 4.

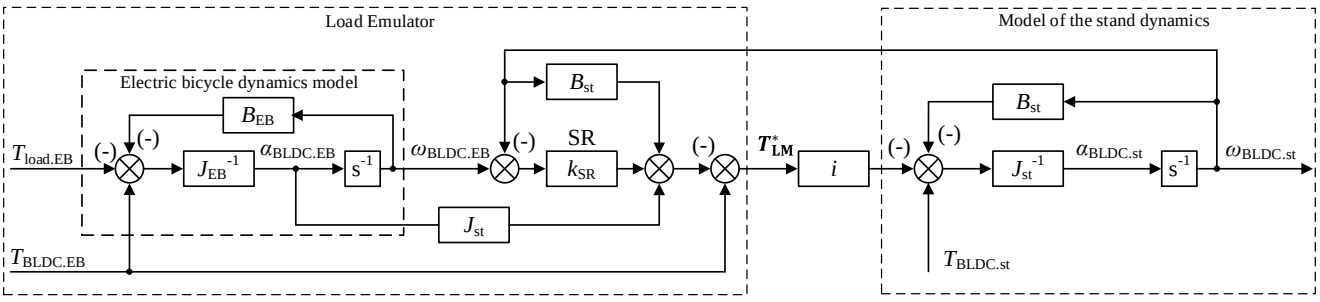


Fig. 3. **Block diagram of the dynamics of stand with EB`s in-wheel motor and a real load torque emulator**

***Source*: compiled by the authors**

Table 4. **Parameters of the equations (11)-(14)**

Parameter	Value
m	100 kg
r_w	0.329 m
k	1.02
γ	2.86°
f_d	0.015
ρ_a	1.23 kg/m^3
A_f	0.5 m^2
c_d	0.22

***Source*: compiled by the authors and from [31]**

The maximum slope, at which the EB can move freely upward, is taken to be 5% that numerically equals: $\gamma = \text{arctg}(5/100) = 2.86°$. The total moment of inertia of the EB with driver reduced to the shaft of the BLDC motor determined by (14) equal to $J_{EB} = 11.11$ kg·m^2.

DEVELOPMENT OF COMPUTER MODELS

Computer model for simulating the EB operation

Fig. 4 shows a computer model of EB operation implemented in MATLAB/Simulink and consists of the following Simscape library subsystems: a BLDC motor model (Permanent Magnet Synchronous Machine), an IN model implemented on MOSFET transistors (Universal Bridge), and a lithium-ion battery model (Battery 1). The static load of the BLDC motor is implemented by the Static Load Subsystem implemented based on equations (10)–(13). The measurement of the energy performance of the drive is implemented by the Power Measurement Subsystem. It calculates the drive efficiency based on information about the voltage and filtered current of the BLDC motor power supply battery B1, as well as the output mechanical power. This subsystem also allows calculating the energy returned to the B1 during regenerative braking of the drive. The Measurement Subsystem measures the electrical variables of the BLDC motor, such as line currents and phase voltages, and calculates the active power consumed by the motor. The Control Subsystem implements a dual-loop system of cascade control of the EB drive.

Fig. 5 depicts a model of a dual-loop cascade control system with an external speed control loop with a proportional speed controller SR_P and an internal current control loop with a proportional-integral current controller CR_PI. The Hall Subsystem reads the rotor position signal and converts it into a switching sequence “pulses” of power switches of the bridge IN. The PWM Subsystem implements a change in the switching logic of the BLDC motor armature windings in the traction and braking modes, and also generates PWM signals based on the output signal of the current controller to control the IN in order to regulate the BLDC motor armature voltages. The Current Measurement Subsystem is used to obtain a current feedback signal in the form of the direct current I equivalent to the value of the linear currents of the BLDC motor, based on the values of the three linear currents measured by the current sensors and the switching sequence “pulses” [30].

Computer model for simulating the stand operation

Fig. 6 shows a computer model of the stand, which is implemented according to the functional diagram shown in Fig. 2 and consists of two parts: the model of the in-wheel motor drive “Electric bicycle drive” and the model of the emulator “Emulator of dynamic and static load”. The model of the in-wheel motor drive differs from the model shown in Fig. 4 only in that the port Tm of the Permanent Magnet Synchronous Machine block receives not a signal from the Static Load Subsystem block, but a load torque signal from the emulator

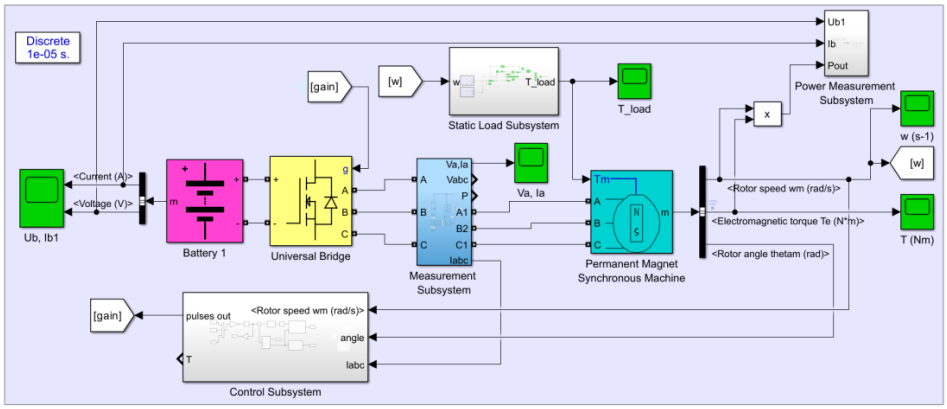


Fig. 4. **Computer model of the EB drive**
***Source*: compiled by the authors**

ISSN 2663-0176 (Print)
ISSN 2663-7731 (Online)

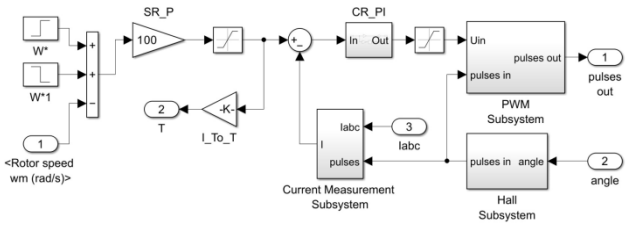


Fig. 5. **Control system of the EB BLDC motor**
***Source*: compiled by the authors**

taking into account the value of the frictional transmission coefficient of 4.44. In addition, in the BLDC motor model of the stand, a lower moment of inertia of the stand drive of 0.5 kg·m² is specified. The load emulator model consists of the following main subsystems: the DC Machine subsystem, which is used as a LM, the bidirectional transistor based Two-Quadrant DC/DC Converter subsystem, the transistor based Two-Quadrant Switch subsystem, and the lithium-ion battery subsystem Battery 2. All of these subsystems are taken from the MATLAB/Simscape library. The mechanical port "w" of the DC Machine subsystem receives the angular velocity setpoint signal of the EB's BLDC motor taking into account the frictional transmission coefficient of 4.44, which simulates their coordinated rotation.

To control the LM, the Load Control Subsystem is developed, which computer model is shown in Fig. 7. The subsystem input receives signals of the angular velocity of the BLDC motor and its electromagnetic torque. The torque value is obtained from the signal at the output of the BLDC motor speed controller, which equivalent to the armature current is proportionally changing by using the torque constant of the BLDC motor (I_To_T block in Fig. 5). The main parts of the Load Control Subsystem are the Torque Emulator subsystem built according to the block diagram shown in Fig. 3, the Static Load Subsystem modeling road load similar to the one that forms the road load in the EB model (Fig. 4), and the closed-loop control system of the LM current with a hysteresis current controller HCR. The load torque generated at the output of the Torque Emulator subsystem is converted into a directly proportional value of the LM current in the Convert block, which takes into account the frictional transmission coefficient and the LM

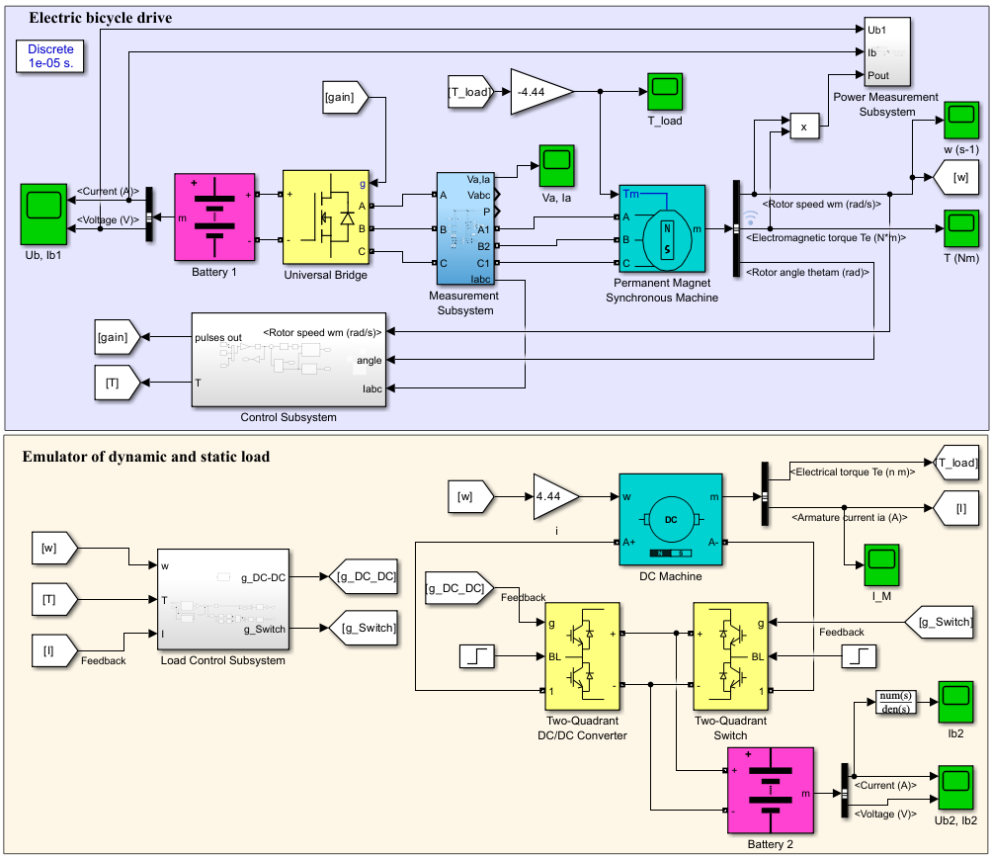


Fig. 6. **Computer model of the stand for studying the EB operation**
***Source*: compiled by the authors**

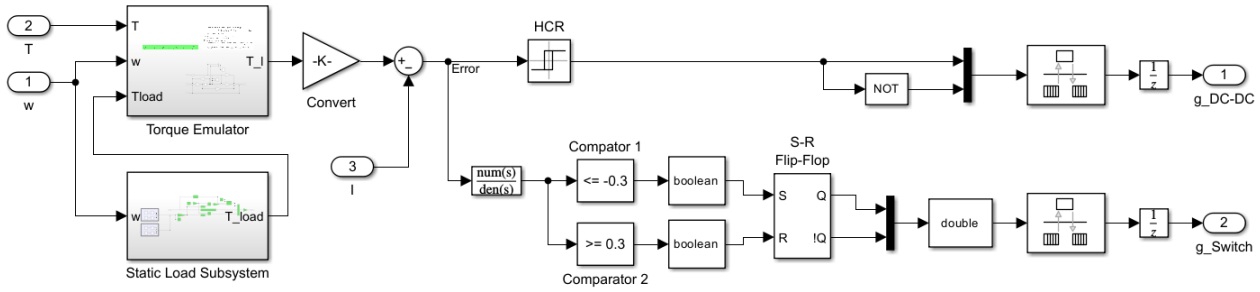


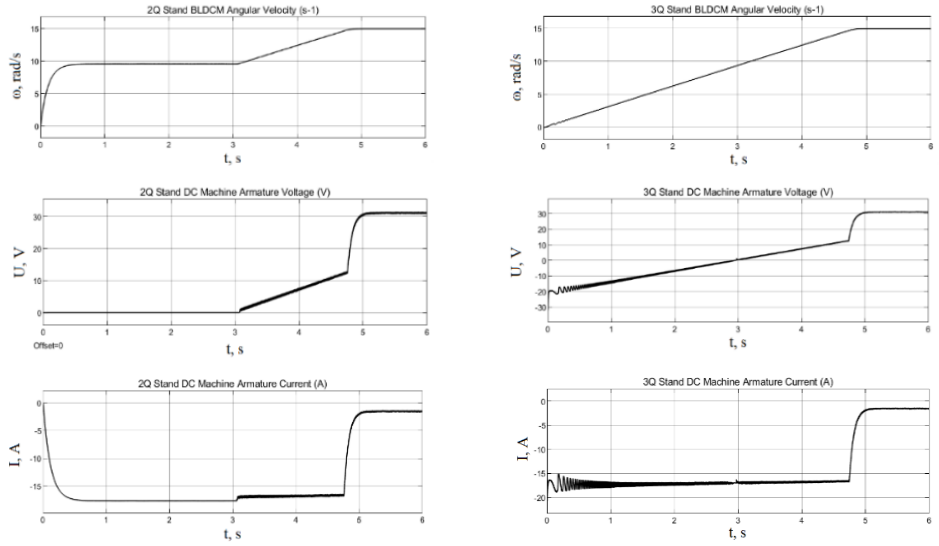
Fig. 7. **EB load emulator control system**
***Source*: compiled by the authors**

torque constant. The obtained value of the LM reference current is compared at the input of the hysteresis current controller with the measured value of the LM current. The HCR output logic signal directly controls, according to the inverse principle, two transistor switches of the Two-Quadrant DC/DC Converter (output g_DC-DC).

Simulation studies have shown that the emulator control system built in this way works correctly at high speeds in the BLDC motor acceleration mode and at all speeds in its regenerative braking mode. It should be noted that in the acceleration mode of the BLDC motor, the LM of emulator operates in the braking mode in the second quadrant of its mechanical characteristics, and in the braking mode of the BLDC motor, the LM of emulator operates in the motor mode in the first quadrant of its mechanical characteristics. However, during the starting of the test bench, at the initial stage of acceleration, as can be seen in Fig. 8a, until the moment of time 3.1 s, the current (torque) of the LM is not regulated. This is due to the fact that in order to provide the necessary braking LM torque, its current must immediately reach the required value of -17 A. For this, the armature voltage must have a negative value. Instead, this voltage has a zero value, since a two-quadrant DC-DC converter cannot provide a negative voltage value. Therefore, the closed loop load system does not work. The LM armature current smoothly increases from zero to -17.6 A, but during this time the stand accelerates to a in-wheel motor angular velocity of 9.2 rad/s. Only after 3.1 s from the stand start, its angular velocity, according to the load emulator, can continue to increase with the specified acceleration, because for this, the LM armature voltage already become positive. Therefore, the load emulator of the stand will continue to work correctly in a closed loop system.

The described situation can be eliminated by ensuring that the two-quadrant DC-DC converter operates in the third quadrant of its volt-ampere characteristic (VAC) at the initial stage of the stand acceleration. This function is assigned to the Two-Quadrant Switch subsystem, which two transistors in one arm can be switched inversely. Such switching is controlled by the S-R Flip-Flop through the g_Switch output in accordance with the value of the LM current regulation error (Fig. 7). This error, through an aperiodic link with a time constant of 0.03 s, which filters a current ripple, is fed to the inputs of two comparators – Comparator 1 and Comparator 2. When the stand is started at low speeds, the current error has a negative value. Accordingly, Comparator 1 turn on that switches the flip-flop and turns on the transistor VT1 of the Two-Quadrant Switch subsystem. The power circuit of the DC-DC converter in this mode takes the form shown in Fig. 9a. Its analysis shows that in this case, Battery 2 is connected in series with the armature and matched in polarity with the LM EMF through the DC-DC converter that is equivalent to its operation in the third quadrant of the VAC. This will provide immediately, from zero speed, the corresponding regulation and maintenance of the LM armature braking current on the level set at the emulator output (Fig. 8b). After the test bench machines will accelerate to a certain angular velocity, the value of the LM EMF will already be sufficient to maintain the set LM braking current. At the same time, the current control error will become positive, Comparator 2 which will turn on and switch the flip-flop to the opposite position, which will accordingly switch the transistors of the Two-Quadrant Switch subsystem. The power circuit of the DC-DC converter in this mode takes the form shown in Fig. 9b. It corresponds to the standard operating mode of the bidirectional DC-DC converter in the second quadrant of its VAC.

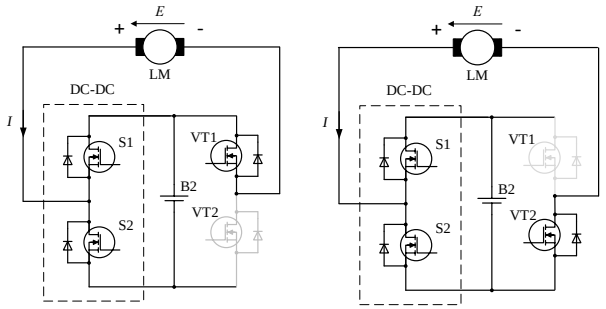
ISSN 2663-0176 (Print)
ISSN 2663-7731 (Online)



a b

Fig. 8. **Time diagrams respectively of the angular velocity of the BLDC motor, the LM armature voltage, and the LM armature current during the start and acceleration of the stand: a – with a two-quadrant DC-DC converter; b – with a three-quadrant DC-DC converter**

***Source*: compiled by the authors**



a b

Fig. 9. **Diagrams of the emulator power circuits in different operatinil modes: a – in the third quadrant of DC-DC converter; b – in the second quadrant of DC-DC converter**

***Source*: compiled by the authors**

RESULTS OF COMPUTER SIMULATION

Testing of the computer model of the EB electric drive was carried out under the following conditions: acceleration of the EB to a speed of 23.7 km/h and its movement at this speed along a straight road, climbing uphill with a 5 % incline, descending a hill with an identical incline, and braking to a complete stop. During descent and braking, the BLDC in-wheel motor control system provides regenerative braking of the BLDC motor.

To assess the correctness of the operation of the proposed stand with the emulator of a real load of the EB, the time diagrams of the main coordinates obtained during simulation of the computer model of the stand (Fig. 10) were compared with the corresponding time diagrams of the coordinates during simulation of the computer model of the EB operation (Fig. 11) under the same driving conditions.

DISCUSSION OF RESULTS

As can be seen in Fig. 10 and Fig.11, the time diagrams for the angular velocity, electromagnetic torque of the BLDC motor, and the power of the electric energy flow from the Battery 1, obtained during simulation for the EB model (Fig. 11a,b,d) and the stand (Fig. 10a,b,h) are visually identical. A numerical comparison of each pair of variables shows that their maximum difference does not exceed 7% of the corresponding nominal value. For better comparison, Fig. 12 shows the angular velocity diagrams of the BLDC motor for the two compared models taken from Fig. 10a and Fig. 11a. Fig. 12 shows that the maximum deviation between the two curves does not exceed 0.25 rad/s, i.e. 1.25% of a maximum angular velocity value of 20 rad/s. This indicates the adequacy of the developed model for emulating static and dynamic loads and the reliable HIL implementation of the stand model. This is also evidenced by the obtained time diagrams of the emulated angular velocity of the BLDC motor and the actual angular velocity of the BLDC motor (Fig. 10d), which are compared at the input of the speed controller SR in the block diagram of the load emulator in Fig. 3.

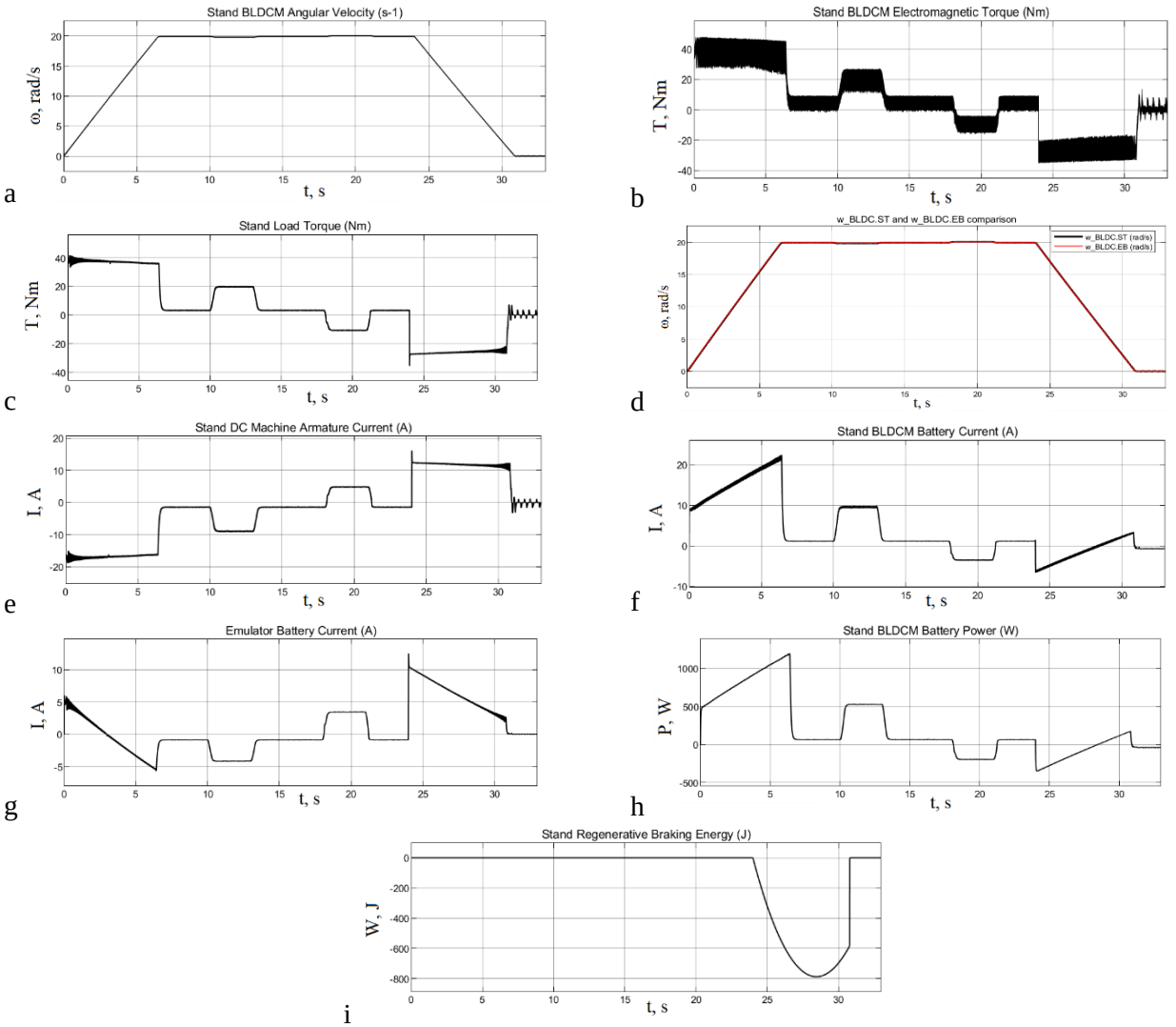


Fig. 10. **Simulation results of the stand model main variables:**
a – BLDC motor angular velocity; b – BLDC motor electromagnetic torque; c – BLDC motor load torque; d – emulated angular velocity and BLDC motor angular velocity; e – LM armature current; f – Battery 1 current; g – Battery 2 current; h – Battery 1 power; i – Battery 1 recovery energy
***Source*: compiled by the authors**

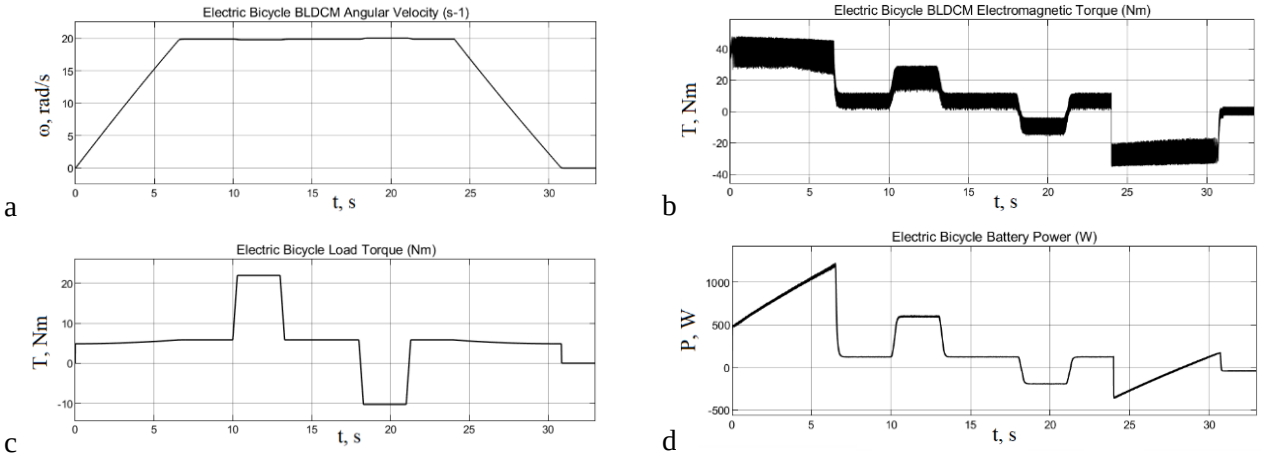


Fig. 11. **Simulation results of the main variables of the EB model:**
a – BLDC motor angular velocity; b – BLDC motor electromagnetic torque; c – road load torque; d – Battery 1 power
***Source*: compiled by the authors**

ISSN 2663-0176 (Print)
ISSN 2663-7731 (Online)

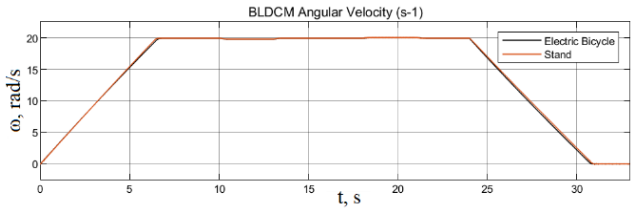


Fig. 12. **Angular velocity time diagrams for the computer models of EB and stand**
***Source*: compiled by the authors**

The time diagram of the load torque applied to the BLDC motor shaft in the stand model (Fig. 10c) is radically different from the corresponding diagram of the load torque for the EB (Fig. 11c). This is because the load torque for the EB only takes into account the road load components determined by expressions (11)-(13), while the dynamic load torque caused by the large moment of inertia of the EV with driver, reduced to the BLDC motor shaft, is reproduced using the BLDC motor model (Permanent Magnet Synchronous Machine). In the case of the stand model, almost the entire dynamic torque is reproduced by the emulator in the form of a load torque for BLDC motor.

The forms of the time diagrams for the currents of the Battery 1 supplied the BLDC motor (Fig. 10f) and the Battery 2 supplied the LM of the emulator (Fig. 10g) are in antiphase, which is typical for HIL systems, since there are energy flows between the EB drive system and the emulator. The different absolute values of these currents are primarily due to the different voltages of the batteries supplying the BLDC motor and LM, as well as energy losses in electric machines and their power converters.

The time diagram of the regenerative braking energy of the BLDC motor, which is transmitted to the Battery 1 (Fig. 10i), shows that at a time moment of approximately 27 s, the recawery energy reaches its maximum of 796 J. Further braking occurs already with energy consumption from the battery. This confirms the fact that regenerative braking is effective only at high and medium drive speeds, while at low speeds it is advisable to use mechanical (hydraulic) brakes [8].

For the purpose of a general comparison of the operation of the computer models of EB with driver and of the stand with load emulation in the formed transport cycle, the power consumed from the Battery 1 in both cases was integrated during the simulation. Accordingly, the following values of energy consumed during the studied cycle were obtained: for the stand with a road load emulator 6685 J and for the EB itself 7173 J. This corresponds to an emulation error of 6.8%.

CONCLUSIONS

As can be seen from the obtained results of computer simulation, the decisions made proved the operability and efficiency of the developed model of the stand with an EB drive and its load emulator using the HIL approach. In its current form, the model can be used to study the operation of the EB electric drive in both traction and braking modes. A separate advantage of the developed model is the possibility of its customization, which allows conducting research under different drive parameters, different EB control by a driver, and under different driving conditions formed by a given road load. At the same time, the emulator correctly forms the corresponding static and dynamic loads on the in-wheel motor in the stand. Based on the results obtained in the work regarding the adequate emulation of the real load for the BLDC motor, in further research, it is planned to manufacture an experimental test banch using HIL testing of a specific EB drive.

REFERENCES

1. Fan, Z. & Harper, C. D. “Congestion and environmental impacts of short car trip replacement with micromobility modes”. *Transp. Res. Part D: Transp. Environ.* 2022; 103: 103173, https://www.scopus.com/pages/publications/85123825004. DOI: https://doi.org/10.1016/j.trd.2022.103173.

2. Ewert, A., Brost, M., Eisenmann, C. & Stieler, S. “Small and light electric vehicles: An analysis of feasible transport impacts and opportunities for improved urban land use”. *Sustainability*. 2020; 12 (19): 8098, https://www.scopus.com/pages/publications/85092629550. DOI: https://doi.org/10.3390/su12198098.

3. Mesimäki, J. & Lehtonen, E. “Light electric vehicles: The views of users and non-users”. *Eur. Transp. Res. Rev.* 2023; 15 (1), https://www.scopus.com/pages/publications/85172356090. DOI: https://doi.org/10.1186/s12544-023-00611-3.

4. Contò, C. & Bianchi, N. “E-bike motor drive: A review of configurations and capabilities”. *Energies*. 2022; 16 (1): 160, https://www.scopus.com/pages/publications/85145648691. DOI: https://doi.org/10.3390/en16010160.

5. Beshta, O. S., Beshta, O. O., Beshta, D., Tkachenko, S., Khalaimov, T. & Skliar, D. “Technologies for increasing the energy efficiency of electric vehicles”. In *2023 IEEE 5th Int. Conf. Modern Electr. Energy*

Syst. (MEES). Kremenchuk, Ukraine. 2023, https://www.scopus.com/pages/publications/85184990620. DOI: https://doi.org/10.1109/MEES61502.2023.10402470.

6. Ostroverkhov, M., Spinul, L. & Veshchykov, H. "Energy conversion efficiency in the electromechanical system with magnetic gear of passenger electric transport rolling stock". *Technol. Audit Prod. Reserves.* 2025; 6 (1), https://www.scopus.com/pages/publications/105028680144. DOI: https://doi.org/10.15587/2706-5448.2025.344863.

7. Karyś, S. & Stawczyk, P. "High-efficiency BLDC motor regenerative braking system with new single-switched transistor control algorithm". *Int. J. Elect. Power Energy Syst.* 2025; 166: 110565, https://www.scopus.com/pages/publications/85218901505. DOI: https://doi.org/10.1016/j.ijepes.2025.110565.

8. Nama, T., Mondal, P., Tripathy, P., Adda, R. & Gogoi, A. K. "Design, modeling and hardware implementation of regenerative braking for electric two-wheelers for hilly roads". *IEEE Access*. 2022; 10: 130602–130618, https://www.scopus.com/pages/publications/85144786611.
DOI: https://doi.org/10.1109/ACCESS.2022.3229597.

9. Mishra, A. K. & Kim, T. "A BLDC motor-driven light plug-in electric vehicle (LPEV) with cost-effective on-board single-stage battery charging system". In *2021 IEEE Transp. Electrific. Conf. Expo (ITEC)*. Chicago, USA. 2021. DOI: https://doi.org/10.1109/ITEC51675.2021.9490066.

10.Li, P., Zhang, Z., Shen, A., Luo, X. & Tang, Q. "Combined unipolar and bipolar PWM for braking control of brushless DC motor". In *2020 Chinese Autom. Congr. (CAC)*. Shanghai, China. Nov. 2020. DOI: https://doi.org/10.1109/CAC51589.2020.9327726.

11. Naseem, H. & Seok, J.-K. "Recent advances in bidirectional converters and regenerative braking systems in electric vehicles". *Actuators*. 2025; 14 (7): 347, https://www.scopus.com/pages/publications/105011476843. DOI: https://doi.org/10.3390/act14070347.

12. Kivanc, O. C. & Ustun, O. "Investigation of regenerative braking performance of brushless direct current machine drive system". *Appl. Sci.* 2021; 11 (3): 1029, https://www.scopus.com/pages/publications/85100115304. DOI: https://doi.org/10.3390/app11031029.

13. Shchur, I. "Bidirectional single-stage Zeta–SEPIC DC-AC converter for traction BLDC motors". In *2022 IEEE 3rd KhPI Week on Advanced Technology*. 2022. 1–6, https://www.scopus.com/pages/publications/85141495005.
DOI: https://doi.org/10.1109/KhPIWeek57572.2022.9916353.

14.Abraham, P. K. & Namboodiry, J. "Ultracapacitor based constant torque regenerative braking system for a brushless DC motor". In *2021 IEEE Int. Power Renew. Energy Conf. (IPRECON)*. Kollam, India. 2021. DOI: https://doi.org/10.1109/IPRECON52453.2021.9640982.

15.Vishnu, S., Dash, A., Praveena Krishna, P. S., Arjun, M. & Jayalakshmi, N. S. "Hybrid control algorithm for BLDC drive involving battery and supercapacitor in E-bikes". In *2022 Int. Virtual Conf. Power Eng. Comput. Control (PECCON)*. Chennai, India. 2022. DOI: https://doi.org/10.1109/PECCON55017.2022.9851060.

16. Kachhwaha, A., Rashed, G. I., Garg, A. R., Mahela, O. P., Khan, B., Shafik, M. B. & Hussien, M. G. "Design and performance analysis of hybrid battery and ultracapacitor energy storage system for electrical vehicle active power management". *Sustainability*. 2022; 14 (2): 776, https://www.scopus.com/pages/publications/85122728412. DOI: https://doi.org/10.3390/su14020776.

17. Pielecha, I. "Energy management system of the hybrid ultracapacitor-battery electric drive vehicles". *Arch. Transp.* 2021; 58 (2): 47–62. https://www.scopus.com/pages/publications/85107920481. DOI: https://doi.org/10.5604/01.3001.0014.8797.

18.Shana, L. P., Gudipalli, A., Fahsyar, P. N. A. & Vaithilingam, C. A. "Performance investigation on BLDC motor and regenerative braking with super-capacitor for electric vehicle application". In *2023 Innov. Power Adv. Comput. Technol. (I-PACT)*. Kuala Lumpur, Malaysia. 2023. DOI: https://doi.org/10.1109/I-PACT58649.2023.10434314.

19. Shchur, I. & Turkovskyi, V. "H–H configuration of modular EV powertrain system based on the dual three-phase BLDC motor and battery-supercapacitor power supply system". *World Electr. Veh. J.* 2023; 14 (7): 173, https://www.scopus.com/pages/publications/85166368531. DOI: https://doi.org/10.3390/wevj14070173.

20. Shchur, I. & Turkovskyi, V. "Open-end winding dual three-phase BLDC motor drive system with integrated hybrid battery-supercapacitor energy storage for electric vehicle". In *2021 IEEE 20th Conf. Mod. Electr. Energy Syst. (MEES)*. Kremenchuk, Ukraine. 2021. 1–6, https://www.scopus.com/pages/publications/85120967586.
DOI: https://doi.org/10.1109/MEES52427.2021.9598697.

ISSN 2663-0176 (Print)
ISSN 2663-7731 (Online)

21. Mohanraj, D., Aruldavid, R., Verma R., Sathiyasekar, K., Abdulwasa, B. B. & Chokkalingam B. “A review of BLDC motor: State of art, advanced control techniques, and applications”. *IEEE Access*. 2022. 10: 54833–54869, https://www.scopus.com/pages/publications/85131708867.
DOI: https://doi.org/10.1109/ACCESS.2022.3175011.

22. Yin, T., Yang, W., Zhang, W., Wu, M., Yu, X. & Han, X. “Research on suppressing commutation torque ripple of BLDCM based on zeta converter”. *Machines*. 2024; 12 (9): 592, https://www.scopus.com/pages/publications/85205098387. DOI: https://doi.org/10.3390/machines12090592.

23. Sa, X., Wu, H., Zhao, G. & Zhao, Z. “Torque ripple reduction in BLDC motors using phase current integration and enhanced zero vector DTC”. *Electronics*. 2025; 14 (15): 2999, https://www.scopus.com/pages/publications/105013382933.
DOI: https://doi.org/10.3390/electronics14152999.

24. Moreno-Suarez, L. E., Morales-Velazquez, L., Jaen-Cuellar, A. Y. & Osornio-Rios, R. A. “Hardware-in-the-loop scheme of linear controllers tuned through genetic algorithms for BLDC motor used in electric scooter under variable operation conditions”. *Machines*. 2023; 11 (6): 663, https://www.scopus.com/pages/publications/85163833933. DOI: https://doi.org/10.3390/machines11060663.

25. Kutsyk, A., Semeniuk, M., Korkosz, M. & Podskarbi, G. “Diagnosis of the static excitation systems of synchronous generators with the use of hardware-in-the-loop technologies”. *Energies*. 2021; 14 (21): 6937, https://www.scopus.com/pages/publications/85117607718. DOI: https://doi.org/10.3390/en14216937.

26. Ibrahim, M., Rassõlkin, A., Vaimann, T. & Kallaste, A. “Overview on digital twin for autonomous electrical vehicles propulsion drive system”. *Sustainability*. 2022; 14 (2): 601, https://www.scopus.com/pages/publications/85122399284. DOI: https://doi.org/10.3390/su14020601.

27. Šlapák, V., Ďurovský, F., Ivan, J. & Hric, M. “Emulation of mechanical loads in electric drives – an overview of methods”. *Power Electron. Drives*. 2023; 8 (1): 53–64, https://www.scopus.com/pages/publications/105003797838. DOI: https://doi.org/10.2478/pead-2023-0004.

28.Kyslan, K., Fedák, V., Ďurovský, F., Sanjeevikumar, P. & Rodič, M. “Design and analysis of torque control for load drive with dynamic emulation”. In *2017 Int. Conf. Optim. Electr. Electron. Equip. (OPTIM) & ACEMP*. Brasov, Romania. 2017. DOI: https://doi.org/10.1109/OPTIM.2017.7974987.

29.Högerl, T., Buberger, J., Schwitzgebel, F. Obkricher, L., Estaller, J. & Hohenegger M. “Battery emulation for battery modular multilevel management (BM3) converters and reconfigurable batteries with series, parallel and bypass function”. In *2021 IEEE Int. Conf. Environ. Elect. Eng. & Ind. and Commercial Power Syst. Eur. (EEEIC / I&CPS Europe)*. Bari, Italy. 2021. DOI: https://doi.org/10.1109/EEEIC/ICPSEUROPE51590.2021.9584557.

30. Shchur, I. Z. & Turkovskyi, V. P. “Integrated system of modular power supply and multilevel control of brushless DC motor for electric vehicles”. *Naukovyi Visnyk Natsionalnoho Hirnychoho Universytetu*. 2020; 6: 68–75, https://www.scopus.com/pages/publications/85099098775. DOI: https://doi.org/10.33271/nvngu/2020-6/068.

31. Siddharth, M. & Rammohan, A. “Development and functional testing of battery management system algorithm for an electric bicycle using hardware in the loop testbench”. *Eng. Res. Express*. 2024; 6: 035357, https://www.scopus.com/pages/publications/85204068370. DOI: https://doi.org/10.1088/2631-8695/ad7559.

Conflicts of Interest: The authors declare that they have no conflict of interest regarding this study, including financial, personal, authorship or other, which could influence the research and its results presented in this article

Received 26.12.2025
Received after revision 12.03.2026
Accepted 19.03.2026

DOI: https://doi.org/10.15276/hait.09.2026.17
УДК: 621.233:629.113.65:519.87

Комп’ютерне моделювання привода колеса електровелосипеда з емуляцією реального навантаження

Щур Ігор Зенонович[1)]
ORCID: https://orcid.org/0000-0001-7346-1463; ihor.z.shchur@lpnu.ua. Scopus Author ID: 36348908300

Лутчин Ігор Юрійович[1)]
ORCID: https://orcid.org/0009-0003-2691-9381; ihor.y.lutchyn@lpnu.ua
Коркош Маріуш [2)]
ORCID: https://orcid.org/0000-0002-9097-0988; mkosz@prz.edu.pl. Scopus Author ID: 56567985000
[1)] Національний університет «Львівська політехніка», вул. Степана Бандери, 12. Львів, 79013, Україна
[2)] Жешівська політехніка, Алея повстанців Варшави, 12. Жешів, 35-029, Польща

АНОТАЦІЯ

Актуальність. Мікромобільні електричні транспортні засоби, приводи яких реалізовано на основі безщіткових двигунів постійного струму, набули поширення в останнє десятиліття. Особливості роботи систем електроприводів цих засобів та бортових систем їх живлення є об'єктом наукових досліджень, які намагаються вирішити такі ключові проблеми як: розширення запасу ходу, зменшення пульсацій електромагнітного моменту, підвищення ефективності рекуперативного гальмування тощо. Огляд літератури показує, що вирішення кожної окремої задачі передбачає застосування двох різних підходів: комп'ютерного моделювання та фізичного експерименту. **Мета і завдання.** Поєднати обидва підходи тестування: проводити експериментальні дослідження з реальними системами транспортних засобів, а вплив на привод дорожнього навантаження та реального динамічного навантаження в перехідних режимах імітувати відповідним емулятором навантаження. Останній складається з апаратної частини, яка формує механічне навантаження на привод, та програмної частини, яка дає змогу імітувати різні задані і повторювані в експериментах режими руху транспортних засобів. **Методи.** У даній роботі Hardware-In-The-Loop підхід застосовано до стенда електровелосипеда, в якому реальне мотор-колесо через фрикційну передачу зв'язане з навантажувальною машиною постійного струму, яка керується двоквадрантним DC-DC перетворювачем. **Результати.** У роботі для керування моментом навантажувальної машини розроблено структуру системи керування емулятором, в якій задаються умови руху електровелосипеда та формуються пов'язані з цими умовами завдання для статичного і динамічного навантажень. Розроблена в середовищі Matlab/Simulink комп'ютерна модель стенда для дослідження привода електровелосипеда дала змогу виявити особливості роботи апаратної частини емулятора навантаження мотор-колеса. Зокрема, під час емуляції динамічного навантаження, пов'язаного з великим моментом інерції привода, під час рушання електровелосипеда з велосипедистом та початкового розгону на невисоких швидкостях двоквадрантний DC-DC перетворювач не здатен забезпечити потрібне значення гальмівного струму навантажувальної машини. Тому довелося забезпечити для вказаного режиму роботу DC-DC перетворювача ще й в третьому квадранті за допомогою додатково введеного двотранзисторного ключа, який дає змогу перемикати роботу DC-DC перетворювача з другого в третій квадрант і навпаки. Розроблено систему керування, яка здійснює таке перемикання. **Висновки.** Порівняння результатів комп'ютерного симулювання роботи привода мотор-колеса електровелосипеда на стенді з емуляцією навантаження з відповідними результатами симулювання роботи цього ж привода в електровелосипеді за однакових умов руху показало розбіжність основних координат руху не вище семи відсотків що підтверджує адекватність емуляції та роботоздатність усіх прийнятих для створення дослідного стенда рішень.

Ключові слова: електровелосипед; дослідний стенд; фізична модель електропривода; безщітковий двигун постійного струму; емулятор реального навантаження; комп'ютерна модель

ABOUT THE AUTHORS



Ihor Z. Shchur - Doctor of Engineering Sciences, Professor, Head of Department of Electromechanical and Electrical Systems. Lviv Polytechnic National University. 12, Stepan Bandery Str. Lviv, 79013, Ukraine.
ORCID: https://orcid.org/0000-0001-7346-1463; ihor.z.shchur@lpnu.ua. Scopus Author ID: 36348908300
***Research field*:** direct drives based on synchronous machines with permanent magnets; electric drives and control systems for electric vehicles; small power renewable energy conversion systems, including photovoltaic and wind turbine; hybrid energy storage systems including batteries and supercapacitors; energy-based mathematical modeling of multi-physics systems; passivity-based controlled systems

Щур Ігор Зенонович - доктор технічних наук, професор, завідувач кафедри Електромеханічних та електротехнічних систем. Національний університет «Львівська політехніка», вул. Степана Бандери, 12. Львів, 79013, Україна



Ihor Y. Lutchyn - PhD student, Department of Electromechanical and Electrical Systems. Lviv Polytechnic National University. 12, Stepan Bandery Str. Lviv, 79013, Ukraine.
ORCID: https://orcid.org/0009-0003-2691-9381; ihor.y.lutchyn@lpnu.ua
***Research field*:** Hardware-In-The-Loop (HIL) systems; regenerative braking of BLDC motors in the light electric vehicles

Лутчин Ігор Юрійович - аспірант кафедри Електромеханічних та електротехнічних систем. Національний університет «Львівська політехніка», вул. Степана Бандери, 12. Львів, 79013, Україна



Mariusz Korkosz - Doctor of Engineering Sciences, Associate Professor, Faculty of Electrical and Computer Engineering, Rzeszow University of Technology, 12, Aleja Powstańców Warszawy, Rzeszow, 35-029, Poland
ORCID: https://orcid.org/0000-0002-9097-0988; mkosz@prz.edu.pl. Scopus Author ID: 56567985000
***Research field*:** 2D/3D modelling; analysis of control; laboratory tests of electrical machines and power systems, in particular, switched reluctance and brushless with permanent magnet for automotive, domestic applications; electric and hybrid drive and aircraft hybrid drive (fault-tolerant, multi-winding, multi-channel drives and their diagnostics, fuel cells).

Коркош Маріуш - доктор технічних наук, професор, факультет Електричної та комп'ютерної інженерії. Жешівська політехніка, Алея Повстанців Варшави, 12. Жешів, 35-959, Польща

ISSN 2663-0176 (Print)
ISSN 2663-7731 (Online)